Entangling dipole-dipole interactions for quantum logic with neutral atoms

Gavin K. Brennen and Ivan H. Deutsch
Center for Advanced Studies, Department of Physics and Astronomy, University of New Mexico, Albuquerque, New Mexico 87131

Poul S. Jessen
Optical Sciences Center, University of Arizona, Tucson, Arizona 85721

(Received 7 October 1999; revised manuscript received 31 January 2000; published 16 May 2000)

We study a means of creating multiparticle entanglement of neutral atoms using pairwise controlled dipole-dipole interactions. For tightly trapped atoms the dipolar interaction energy can be much larger than the photon scattering rate and substantial coherent evolution of the two-atom state can be achieved before decoherence occurs. Excitation of the dipoles can be made conditional on the atomic states, allowing for deterministic generation of entanglement. We derive selection rules and a figure of merit for the dipole-dipole interaction matrix elements, for alkali atoms with hyperfine structure and trapped in localized center of mass states. Different protocols are presented for implementing two-qubit quantum logic gates such as the controlled-phase and swap gates. We analyze the error probability of our gate designs, finite due to decoherence from cooperative spontaneous emission and coherent couplings outside the logical basis. Outlines for extending our model to include the full molecular interactions potentials are discussed.

PACS number(s): 03.67.Lx, 32.80.Qk, 32.80.Lg, 32.80.Pj

I. INTRODUCTION

The ability to coherently manipulate multiparticle entanglement represents the ultimate quantum control of a physical system and opens the door to a wide variety of fundamental studies and applications, ranging from improvements in precision measurement [1] to quantum simulation [2,3] and quantum computation [4]. Several physical realizations have been proposed in quantum optics, including ion traps [5] and cavity QED [6], and ''engineered'' entanglement has been demonstrated in the laboratory for both of these systems [7,8]. Entangling unitary transformations have been implemented in liquid-state NMR on pseudopure states of nuclear spins in small organic molecules [9], though true entanglement has not yet been produced in these thermal samples [10]. Proposals have been made also for a number of condensed-matter implementations, such as quantum dots [11], superconducting quantum interference devices (SQUIDs) [12], and coupled spin resonance of dopants in a silicon lattice [13]. All these implementations must contend with the conflict inherent to open quantum systems. Entangling unitary operations must provide strong coherent coupling of the atoms or spins with each other and also with the external driving field, while shielding the system from the noisy environment that leads to decoherence.

Recently we identified a new method for producing multiparticle entangled states of cold trapped neutral atoms [14] (see also [15–17]). This system offers several advantages for quantum information processing. In general, neutral atoms in their electronic ground state couple extremely weakly both to each other and to the environment. Interatomic couplings can, however, be created *on demand* by external fields, which excite two-atom resonances such as those arising from electric dipole-dipole interactions [14], by ground-state collisions [15], or by real photon exchange [16,17]. The ability to turn interactions ''on'' only when needed is highly advantageous because it reduces coupling to the environment and the spread of errors among atoms. To create entanglement one must accurately control both the atomic internal and external degrees of freedom so that the interatomic coupling can be applied in a coherent manner and with high fidelity.

In this paper we consider the creation of entanglement via resonantly induced dipole-dipole interactions between atoms in tightly confining traps, such as those produced by optical lattices [18] or magnetic traps [19]. Our goal is to establish some general features that can be applied in a variety of settings. Experimental details will be omitted except to give order of magnitude estimates where appropriate—a more complete description of our proposal will be published elsewhere [20]. We begin with a discussion in Sec. II of the dipole-dipole interaction, establishing the ''figure of merit'' for entangling interactions and the selection rules for transitions between internal and external states for two atoms in a confining trap. In Sec. III we demonstrate the flexibility available for implementing quantum logic in this system by presenting three different two-qubit logic protocols and estimate the figure of merit for each due to spontaneous emission. A major deficit in the present analysis is the omission of inelastic collision channels from the model [21]. Such a task has considerable challenges, especially when one includes the complex internal structure of the atoms in the molecular potentials [22]. In Sec. IV we give an outlook toward this and other future research.

II. THE DIPOLE-DIPOLE INTERACTION

The dipole-dipole interaction depends both on the internal electronic states of the atoms as dictated by the tensor nature of the interaction, and the external motional states that determine the relative coordinate probability distribution of the dipoles. We consider a system of two atoms trapped in separate harmonic potentials, interacting coherently with a classical field and with each other via the dipole-dipole interaction. Decoherence may occur via cooperative spontaneous

emission. We will begin with a discussion of the simplest case, two two-level atoms. This will establish the basic features we will exploit for entangling neutral atoms. We then consider a more realistic multilevel structure associated with alkali atoms, the most readily cooled and trapped atomic species. We seek expressions for the interaction matrix elements and the resulting selection rules.

A. Two-level atoms

Consider two two-level atoms at fixed points separated by distance r, with ground and excited states $|g\rangle$, $|e\rangle$, interacting with a laser field at frequency ω_L. After tracing over the vacuum modes in the Born-Markov approximation, the effective non-Hermitian Hamiltonian is [23]

$$H_{\rm eff}=H_A+H_{\rm AL}+H_{dd}, \tag{1}$$

where the atomic Hamiltonian and the atom-laser interaction are

$$H_A=\left(-\hbar\Delta-i\frac{\Gamma}{2}\right)(D_1^\dagger D_1+D_2^\dagger D_2), \tag{2}$$

$$H_{\rm AL}=-\frac{\hbar\Omega}{2}(D_1^\dagger+D_2^\dagger+{\rm H.c.}). \tag{3}$$

Here, $\Delta=\omega_L-\omega_{eg}$ is the laser detuning, Γ is the excited state decay rate, Ω is the Rabi frequency, and $D^\dagger=|e\rangle\langle g|$ is the dimensionless dipole raising operator for each atom. The dipole-dipole coupling interaction Hamiltonian is of the form

$$H_{dd}=\left(V_c-i\frac{\hbar\Gamma_c}{2}\right)(D_1^\dagger D_2+D_2^\dagger D_1), \tag{4}$$

where V_c is the coupling strength that depends explicitly on r, and Γ_c is the collective contribution to the decay rate.

In order to analyze this system we must choose an appropriate basis of states. There are two natural choices: the atomic and molecular bases. In the atomic case one considers product states of internal dynamics and center of mass motion. In the molecular case one considers eigenstates of the dipole-coupled two-atom Hamiltonian H_A+H_{dd} in the Born-Oppenheimer approximation. Both bases form a complete set of states and thus allow for a full description of the physics, though the transparency of the model may be greater with one or the other, depending on the nature of the problem. For low atomic densities the atomic basis is convenient (see, for example, [24]), whereas at high densities where collisions play a dominate role the molecular basis is more natural (see, for example, [21]). For the simple example of two two-level atoms the relation between these bases is seen immediately by a diagonalization of H_A+H_{dd}, yielding ''molecular eigenstates'' (see also [25])

$$|g_1,g_2\rangle,|\psi_\pm\rangle=\frac{|e_1g_2\rangle\pm|g_1e_2\rangle}{\sqrt{2}},|e_1e_2\rangle. \tag{5}$$

In this basis the Hamiltonian is $H_{\rm eff}=H_0+H_{\rm AL}$, with

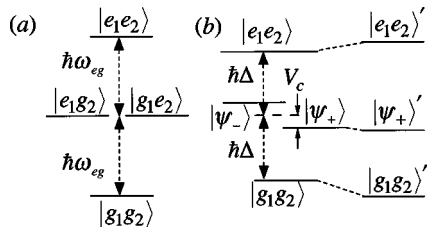

FIG. 1. Internal energy levels for two atoms. (a) The bare energy eigenbasis showing degenerate states with one photon excitation. (b) The two-atom picture in the rotating frame at field detuning Δ with dipole-dipole splitting of the symmetric and antisymmetric states. The primed states to the right are the dressed atomic states including the sum of the light shift and dipole-dipole potentials (not to scale).

$$H_0=-\hbar(\Delta+i\Gamma/2)\{2|e_1e_2\rangle\langle e_1e_2|+|\psi_+\rangle\langle\psi_+|+|\psi_-\rangle\langle\psi_-|\}+(V_c-i\hbar\Gamma_c/2)\{|\psi_+\rangle\langle\psi_+|-|\psi_-\rangle\langle\psi_-|\}, \tag{6a}$$

$$H_{\rm AL}=\frac{\hbar\Omega}{\sqrt{2}}(|g_1g_2\rangle\langle\psi_+|+|e_1e_2\rangle\langle\psi_+|+{\rm H.c.}). \tag{6b}$$

The symmetric state $|\psi_+\rangle$ is super-radiant with linewidth $\Gamma+\Gamma_c$, and couples to $|g_1g_2\rangle$ and $|e_1e_2\rangle$ with Rabi frequency $\sqrt{2}\Omega$. The state $|\psi_-\rangle$ is subradiant with linewidth $\Gamma-\Gamma_c$. The states $|\psi_\pm\rangle$ may be denoted by molecular spectroscopic notation with eigenvalues Σ, Π, etc., depending on the orientation of the dipoles with respect to the direction of the internuclear axis [25]. This is implicit in the definition of the coupling constant V_c,

Given this Hamiltonian we can calculate the dressed–ground-state energy by treating $H_{\rm AL}$ as a perturbation to second order. We find

$$E_{gg}=\frac{\hbar\Omega^2/2}{(\Delta-V_c/\hbar)+i(\Gamma+\Gamma_c)/2}. \tag{7}$$

When $\Delta\gg V_c,\Gamma$ the saturation is *independent* of the dipole-dipole interaction, which is equivalent to a separation between the internal state dynamics and the external degrees of freedom. In this limit

$$E_{gg}\approx s(\hbar\Delta-i\hbar\Gamma/2)+s(V_c-\hbar\Gamma_c/2), \tag{8}$$

where $s\approx\Omega^2/(2\Delta^2)$ is the single atom saturation parameter. The first term in Eq. (8) represents the sum of the single atom light shifts and the photon scattering rate. The second term, $H_{dd}\equiv s(V_c-i\hbar\Gamma_c/2)$, is the two-atom cooperative dipole-dipole effect on the ground-state perturbation, with sV_c giving the coherent level-shift and $s\Gamma_c$ the cooperative contribution to the spontaneous emission rate. The level shifts of the molecular eigenstates in this perturbative limit are shown in Fig. 1. We define a *figure of merit* κ for the dipole-dipole interaction as

$$\kappa\equiv\frac{{\rm Re}(H_{dd})}{2|{\rm Im}(E_{gg})|}=\frac{V_c}{\hbar(\Gamma+\Gamma_c)}\equiv\frac{V_c}{\hbar\Gamma_{\rm tol}}. \tag{9}$$

This represents the rate at which the cooperative phase shift is accumulated compared to the total rate of decay due to spontaneous emission $\Gamma_{\rm tot}$ and is the central parameter that measures the quality of the interaction. Note that in the high detuning limit this figure is *independent* of the saturation of the atomic populations.

A simple scaling argument shows the plausibility of using atomic dipole-dipole interactions to construct entangling unitaries. In the near field $V_c \sim d^2/r^3$, where d is the mean induced dipole moment per atom. In contrast, the total spontaneous emission rate can be no larger than the Dicke superradiant rate equal to twice the single atom decay rate, $\hbar\Gamma \sim k^3 d^2$, where k is the photon wave number. Thus, the figure of merit scales as $\kappa \sim (kr)^{-3}$, which is potentially quite large for tight traps, deep in the Lamb-Dicke regime. In order to evaluate the proportionality constant, we must consider a more realistic model for the system as discussed in the next section.

B. Multilevel atoms

Consider now two alkali atoms with nuclear spin I, center of mass positions $\mathbf{r}_1$, $\mathbf{r}_2$, and excited on the $D2$ transition, $|S_{1/2}(F)\rangle \leftrightarrow |P_{3/2}(F')\rangle$, where F and F' belong to the ground- and excited-state hyperfine manifolds. The atoms interact with the vacuum field and a classical monochromatic laser field $\mathbf{E} = \mathrm{Re}\,(E_L \boldsymbol{\varepsilon}_L(\mathbf{x}) e^{-i\omega_L t})$, with amplitude E_L and local polarization given by $\boldsymbol{\varepsilon}_L(\mathbf{x})$. The multilevel generalization of Eqs. (1)–(4) for the effective atom-laser Hamiltonian, together with a dipole-dipole interaction between atoms are [26],

$$H_{\rm AL} = -\hbar\left(\Delta + i\frac{\Gamma}{2}\right)(\mathbf{D}_1^\dagger \cdot \mathbf{D}_1 + \mathbf{D}_2^\dagger \cdot \mathbf{D}_2) \tag{10a}$$

$$-\frac{\hbar\Omega}{2}[\mathbf{D}_1^\dagger \cdot \boldsymbol{\varepsilon}_L(\mathbf{r}_1) + \mathbf{D}_2^\dagger \cdot \boldsymbol{\varepsilon}_L(\mathbf{r}_2) + \mathrm{H.c.}], \tag{10b}$$

$$H_{dd} = V_{dd} - i\frac{\hbar\Gamma_{dd}}{2} = -\frac{\hbar\Gamma}{2}[\mathbf{D}_2^\dagger \cdot \vec{\vec{\mathbf{T}}}(k_L r) \cdot \mathbf{D}_1 + \mathbf{D}_1^\dagger \cdot \vec{\vec{\mathbf{T}}}(k_L r) \cdot \mathbf{D}_2], \tag{10c}$$

where the relevant Rabi frequency is given by $\Omega = \langle J' = \frac{3}{2} \| d \| J = \frac{1}{2} \rangle E_L/\hbar$, having used the Condon and Shortley [27] convention for reduced dipole matrix elements, and the dimensionless vector dipole raising operator is defined as

$$\mathbf{D}^\dagger = \sum_{F'} \frac{P_{F'} \mathbf{d} P_F}{\langle J' \| d \| J \rangle} = \sum_{F'} o_{F'F} \sum_{q=-1}^{1} \sum_{M_F} \mathbf{e}_q^* C^{F,1,F'}_{M_F,q,M_F+q} |F', M_F+q\rangle\langle F, M_F|, \tag{11a}$$

$$o_{F'F} = \sqrt{(2J'+1)(2F+1)} \begin{Bmatrix} F' & I & J' \\ J & I & F \end{Bmatrix}. \tag{11b}$$

Here $P_{F',F}$ are projectors on the excited and ground manifolds, $\mathbf{e}_q$ are the spherical basis vectors, $c^{F,l,F'}_{M_F,q,M_F+q}$ is the Clebsch-Gordan coefficient for the electric dipole transition $|F, M_F\rangle \rightarrow |F', M_F+q\rangle$, and $o_{F'F}$ is the relative oscillator strength of each hyperfine transition as set by the $6j$ symbol. The second rank tensor, $\vec{\vec{\mathbf{T}}} = \vec{\vec{\mathbf{f}}} + i\vec{\vec{\mathbf{g}}}$, describes the strength of the two-atom interaction as a function of atomic separation $r = |\mathbf{r}_1 - \mathbf{r}_2|$,

$$\vec{\vec{\mathbf{f}}}(k_L r) = \frac{2}{3}\left[(\vec{\vec{\mathbf{1}}} - \hat{\mathbf{r}}\hat{\mathbf{r}})\frac{\cos(k_L r)}{k_L r} - (\vec{\vec{\mathbf{1}}} - 3\hat{\mathbf{r}}\hat{\mathbf{r}}) \times \left(\frac{\sin(k_L r)}{(k_L r)^2} + \frac{\cos(k_L r)}{(k_L r)^3}\right)\right], \tag{12a}$$

$$\vec{\vec{\mathbf{g}}}(k_L r) = \frac{3}{2}\left[(\vec{\vec{\mathbf{1}}} - \hat{\mathbf{r}}\hat{\mathbf{r}})\frac{\sin(k_L r)}{k_L r} + (\vec{\vec{\mathbf{1}}} - 3\hat{\mathbf{r}}\hat{\mathbf{r}}) \times \left(\frac{\cos(k_L r)}{(k_L r)^2} - \frac{\sin(k_L r)}{(k_L r)^3}\right)\right]. \tag{12b}$$

The Hermitian part of the effective interaction Hamiltonian V_{dd} determines the dipole-dipole energy level shift. The anti-Hermitian part Γ_{dd} gives rise to cooperative spontaneous emission so that the total decay rate is given by the expectation value of $\Gamma_{\rm tot} = \Gamma(\mathbf{D}_1^\dagger \cdot \mathbf{D}_1 + \mathbf{D}_2^\dagger \cdot \mathbf{D}_2) + \Gamma_{dd}$. In the near field (the limit $k_L r \rightarrow 0$) one finds that the real and imaginary parts of the dipole-dipole Hamiltonian are $V_{dd} \rightarrow [\mathbf{d}_1 \cdot \mathbf{d}_2 - 3(\hat{\mathbf{r}} \cdot \mathbf{d}_1)(\hat{\mathbf{r}} \cdot \mathbf{d}_2)]/r^3$, the quasistatic dipole-dipole interaction, and $\Gamma_{dd} \rightarrow \Gamma(\mathbf{D}_1 \cdot \mathbf{D}_2^\dagger + \mathbf{D}_2 \cdot \mathbf{D}_1^\dagger)$, the Dicke super- (or sub) radiant interference term for in (or out of) phase dipoles.

As in the two-level case described in Sec. II A, we must choose an appropriate basis. For atoms with both fine and hyperfine structure the molecular basis has a very complex description [22]. To develop some intuitive understanding we will restrict our attention to the atomic basis, and defer discussion of the more general problem to Sec. IV. Consider then a product state with the two atoms in the same internal state, $|\Psi\rangle = |\psi_{\rm int}\rangle_1 |\phi_{\rm ext}\rangle_1 \otimes |\psi_{\rm int}\rangle_2 |\xi_{\rm ext}\rangle_2$, each with its mean dipole moment vector oscillating along the spherical basis vector $\mathbf{e}_q$. Under this circumstance the figure of merit for coherent dipole-dipole level shift defined in Eq. (9) can be generalized to the multilevel case through Eq. (10),

$$\kappa = \frac{\langle V_{dd}\rangle}{\langle \hbar\Gamma_{\rm tot}\rangle} = \frac{-\hbar\Gamma\langle D_q^\dagger D_q\rangle_{\rm int}\langle f_{qq}\rangle_{\rm ext}}{2\hbar\Gamma\langle D_q^\dagger D_q\rangle_{\rm int}(1 + \langle g_{qq}\rangle_{\rm ext})} = \frac{-\langle f_{qq}\rangle_{\rm ext}}{2(1 + \langle g_{qq}\rangle_{\rm ext})}. \tag{13}$$

This factor depends only on *geometry*: the external states and the direction of polarization of the oscillating dipoles. It is

independent of the strength of the dipole, since the same matrix element for the atoms' internal states appears both in the numerator and denominator. The average over the external state is carried out with respect to the relative coordinate probability density, having traced over the center of mass of the two-atom system.

We will focus here on weak excitation of the dipoles. As in Sec. II A, adiabatic elimination of the excited states follows from second-order perturbation theory in the limit of small saturation of the atomic transitions. We will further assume that the detuning is large compared to the excited state level shifts over the *entire range* of the relative coordinate probability distribution. This is exactly the approximation used to obtain Eq. (8). In that case, the light shift contribution to the level shift factors out as in Eq. (8), and the effective cooperative dipole-dipole Hamiltonian on the ground-state manifold is [24]

$$H_{dd}=V_{dd}-i\frac{\hbar\Gamma_{dd}}{2}$$
$$=-s\frac{\hbar\Gamma}{2}\sum_{q,q'=-1}^{1}(f_{qq'}+ig_{qq'})\{[\mathbf{D}_1\cdot\boldsymbol{\varepsilon}_L^*(\mathbf{r}_1)](\mathbf{D}_1^\dagger\cdot\mathbf{e}_q)$$
$$\times(\mathbf{D}_2\cdot\mathbf{e}_{q'}^*)[\mathbf{D}_2^\dagger\cdot\boldsymbol{\varepsilon}_L(\mathbf{r}_2)]+\text{H.c.}\}. \quad (14)$$

The interaction tensor is written here in the spherical basis,

$$f_{qq'}(k_Lr)=[n_0(k_Lr)\delta_{qq'}+(-1)^q n_2(k_Lr)$$
$$\times Y_2^{q'-q}(\theta-\phi)\sqrt{6\pi/5}c^{1,1,2}_{-q,q',-q+q'}],$$
$$g_{qq'}(k_Lr)=[j_0(k_Lr)\delta_{qq'}+(-1)^q j_2(k_Lr)$$
$$\times Y_2^{q'-q}(\theta-\phi)\sqrt{6\pi/5}c^{1,1,2}_{-q,q',-q+q'}], \quad (15)$$

where $j_m(n_m)$ are the mth-order spherical Bessel (Neumann) functions and Y_l^{ln} (θ,ϕ) are the spherical angles of the relative coordinate $\mathbf{r}$. The zeroth-order Bessel and Neumann functions account for retardation in the dipole-dipole interaction and will be neglected below.

Physically, Eq. (14) represents a four-photon process: absorption of a laser photon by one atom followed by coherent exchange of the excitation between the atoms via a virtual photon emission and absorption, and finally stimulated emission of a laser photon returning both atoms to the ground state. Because the virtual photon can be emitted in any direction it is not an eigenstate of angular momentum with respect to the space-fixed quantization axis of the atoms. The quantum numbers q and q' represent two of the possible projections of its angular momentum on that axis. Examples of these fundamental photon exchange processes are shown in Fig. 2.

We are left to consider the geometry of the trapping potentials, resulting external coordinate wave functions, and the polarization of the oscillating dipoles. For deep traps we can approximate the motional states as harmonic oscillators. For the particular case of an isotropic trap, the spherical symmetry allows explicit evaluation of the interaction matrix elements. Consider two atoms in a common well, each described by a set of radial and angular momentum vibrational quantum numbers $|n,l,m\rangle$ [28], with energy $E_{nl}=2n+l+3/2$, degeneracy $g_{nl}=(2n+l+1)(2n+l+2)/2$, and an internal state denoting one of the ground magnetic sublevels of a given hyperfine state $|F,M_F\rangle$. One can decompose the product state of the two isotropic harmonic oscillators into relative and center of mass states, which then can be used to find analytic expressions for the matrix elements with a general tensor coupling. Given dipoles excited with polarization $\mathbf{e}_\lambda$, we can evaluate the matrix element with respect to the internal degree of freedom,

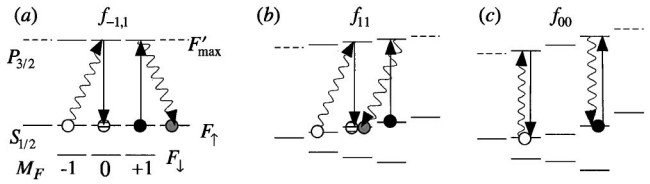

FIG. 2. Fundamental photon exchange processes allowed in the dipole-dipole interaction. Solid lines indicate stimulated emission and absorption of a laser photon; wavy lines indicate emission and absorption of a virtual photon responsible for the exchange interaction. The contributing component of the dipole-dipole interaction tensor, $f_{qq'}$, from Eq. (15) is indicated above. The black and white dots represent the initial state of the two interacting atoms; the gray and striped dots represent the final states, respectively. (a) With degenerate ground states, transitions that conserve neither M_{F1}, M_{F2} nor total M_F are allowed. (b) Under a linear Zeeman shift only processes conserving total M_F are resonant. (c) A nonlinear Zeeman or ac-Stark shift will constrain the interaction to return both atoms to their initial states.

$$\langle F,M_{F1};n_1l_1m_1|\otimes\langle F,M_{F2};n_2l_2m_2|V_{dd}|F,M'_{F1};n'_1l'_1m'_1\rangle$$
$$\otimes|F,M'_{F2};n'_2l'_2m'_2\rangle$$
$$=\sum_{q,q'=-1}^{1}(-1)^q c^{1,1,2}_{-q,q',-q+q'}\sqrt{6\pi/5}$$
$$\times\langle n_1l_1m_1|\otimes\langle n_2l_2m_2|V(r)Y_2^{q'-q}(\theta,\phi)|n'_1l'_1m'_1\rangle$$
$$\otimes|n'_2l'_2m'_2\rangle(c^{F,1,F'}_{M'_{F2},\lambda,M'_{F2}+\lambda}c^{F',1,F}_{M'_{F2}+\lambda,-q',M_{F2}}$$
$$\times c^{F,1,F'}_{M'_{F1},q,M_{F1}+q}c^{F',1,F}_{M'_{F1}+q,-\lambda,M_{F1}}$$
$$+c^{F,1,F'}_{M'_{F1},\lambda,M'_{F1}+\lambda}c^{F',1,F}_{M'_{F1}+\lambda,-q',M_{F1}}$$
$$\times c^{F,1,F'}_{M'_{F2},q,M'_{F2}+q}c^{F',1,F}_{M'_{F2}+q,-\lambda,M_{F2}}), \quad (16)$$

where $V(r)=-s\hbar\Gamma n_2(k_Lr)/2\sim 1/\eta^3$, having neglected the radiation term $n_0(k_Lr)\sim 1/\eta$ for $\eta\ll 1$.

The Clebsch-Gordan coefficients of the four-photon process in Eq. (16) dictate selection rules for the internal states,

$$M_{F1}+M_{F2}=(M'_{F1}+M'_{F2})+(q-q'). \quad (17)$$

We see that neither M_{F1}, M_{F2}, nor the total $M_{F1}+M_{F2}$ is a conserved quantity. The fact that these are not good quantum

numbers can be seen immediately from the form of the interaction Hamiltonian, Eq. (10b), which is neither a scalar with respect to rotations by hyperfine operators $\hat{\mathbf{F}}_1$, $\hat{\mathbf{F}}_2$, nor $\hat{\mathbf{F}}_1+\hat{\mathbf{F}}_2$. Classically this is reflected in the fact that the dipole-dipole interaction is *not a central force*, and therefore the angular momentum of two classical dipoles about their center of mass is not a conserved quantity. Generally, internal angular momentum can be converted to rotational energy of the molecule if the atoms have multiply degenerate energy levels. An example of a quantum mechanical process that does not conserve $M_{F1}+M_{F2}$ in shown in Fig. 2(a). Techniques to conserve the total and individual atomic internal quantum numbers by, e.g., breaking ground-state degeneracy [Figs. 2(b) and 2(c)], are discussed in Sec. III.

To evaluate the external-state matrix element in Eq. (16) we first expand the uncoupled angular momentum basis for the motional states $|l_1 m_1\rangle\otimes|l_2 m_2\rangle$ in terms of the coupled states $|\lambda,\ \mu\rangle$ for total angular momentum λ and projection μ according to the usual vector addition rules, so that

$$\langle n_1 l_1 m_1|\otimes\langle n_2 l_2 m_2|V(r)Y_2^{m_r}(\theta,\phi)|n_1' l_1' m_1'\rangle\otimes|n_2' l_2' m_2'\rangle$$
$$=\sum_{\lambda,\lambda'}\sum_{\mu,\mu'} c^{l_1,l_2,\lambda}_{m_1,m_2,\mu} c^{l_1',l_2',\lambda'}_{m_1',m_2',\mu'}\langle n_1 l_1 n_2 l_2;\lambda\mu|V(r)$$
$$\times Y_2^{m_r}(\theta,\phi)|n_1' l_1' n_2' l_2';\lambda'\mu'\rangle. \tag{18}$$

Borrowing a technique from nuclear physics due to Moshinsky [29] we express coupled isotropic harmonic oscillator wave functions for the two atoms in the product basis of center of mass oscillator states $|NL\rangle$ and relative coordinate oscillator states $|nl\rangle$ as summarized in [30]. The matrix element in Eq. (18) can then be written

$$\langle n_1 l_1 n_2 l_2;\lambda\mu|V(r)Y_2^{m_r}(\theta,\phi)|n_1' l_1' n_2' l_2';\lambda'\mu'\rangle$$
$$=\sum_{nNlLl'}\langle n_1 l_1 n_2 l_2,\lambda|nl,NL,\lambda\rangle$$
$$\times\langle n'l',NL,\lambda'|n_1' l_1' n_2' l_2',\lambda'\rangle$$
$$\times(-1)^{L+\lambda'+l}\sqrt{\frac{5(2\lambda'+1)(2l+1)}{(4\pi)}}$$
$$\times c^{\lambda',2,\lambda}_{\mu',m_r,\mu} c^{l,2,l'}_{0,0,0}\begin{Bmatrix} l & \lambda & L\\ \lambda' & l' & 2\end{Bmatrix}$$
$$\times\sum_{p=(l+l')/2}^{(l+l')/2+n+n'} B(nl,n'l',p)I_p[V(r)], \tag{19}$$

with restrictions on the quantum numbers to conserve the total mechanical energy,

$$E_{\rm tot}=E_1+E_2=E_1'+E_2'=E_{CM}+E_{\rm rel}=E_{CM}'+E_{\rm rel}' \tag{20a}$$

$$\Rightarrow n'=n+n_1'+n_2'-n_1-n_2+(l_1'+l_2'-l_1-l_2+l-l')/2. \tag{20b}$$

In Eq. (19) $\langle n_1 l_1 n_2 l_2,\lambda|nl,NL,\lambda\rangle$ are ''Moshinsky brackets'' that are tabulated real coefficients found using recursion relations, $B(nl,n'l',p)$ are radial function expansion coefficients given in [31], and $I_p[V(r)]$ are the Talmi integrals given in [30]. The Moshinsky brackets satisfy conservation of parity of the wave function, i.e., $(-1)^{l_1+l_2}=(-1)^{l+L},(-1)^{l_1'+l_2'}=(-1)^{l'+L}$ and coupling with a rank-two tensor restricts angular momentum quantum numbers to $l'=l,\ l\pm 2$. The Clebsch-Gordan coefficients in Eq. (18) impose the constraint $\mu=m_1+m_2$, and $\mu'=m_1'+m_2'$, while Eq. (19) requires $\mu-\mu'=m_r$. Thus, the selection rule for a tensor coupling between isotropic harmonic oscillator states is

$$m_1'+m_2'+m_r=m_1+m_2. \tag{21}$$

This is the analog of Eq. (17), now with respect to the atomic motional states. The quantum number m_r can be interpreted as the projection of the net angular momentum of the exchanged virtual photons responsible for dipole-dipole interactions [i.e., $m_r=\pm(q-q')$]. The deficit Δq is converted to mechanical rotation of the molecule, consistent with overall energy conservation, Eq. (20).

In addition to degenerate couplings resulting in changes in internal states as described above, for atoms in excited vibrational modes of a common spherical well there are further degeneracies and couplings allowed by the energy conservation law Eq. (20a) and selection rule Eq. (21). For instance, the product state of two atoms, each with one quanta of vibration along z, can couple to the seven dimensional degenerate subspace of two quanta shared between the two atoms,

$$|n_1 l_1 m_1\rangle\otimes|n_2 l_2 m_2\rangle=\{|010\rangle\otimes|010\rangle,|01-1\rangle\otimes|011\rangle,|011\rangle$$
$$\otimes|01-1\rangle,|020\rangle\otimes|000\rangle,|000\rangle$$
$$\otimes|020\rangle,|100\rangle\otimes 000\rangle,|000\rangle\otimes 100\rangle\}. \tag{22}$$

All of these features must be accounted for if we are to utilize the dipole-dipole interaction for coherent quantum state manipulation and logic gates, as we consider in the next section.

III. QUANTUM LOGIC GATES

A. General considerations

The dipole-dipole interaction discussed in Sec. II can bring about coherent interactions between neutral atoms. A useful paradigm to generate an arbitrary unitary evolution of a many-body system is the ''quantum circuit'' defined by a series of logic gates acting on a set of two-level quantum systems (qubits) [4], here the trapped atoms with pure states identified as the logical-$|0\rangle$ and $|1\rangle$. A crucial component is the two-qubit logic gate whereby the state of one atom (called the target) is evolved conditional on the logical state of the other (called the control). A familiar example is the ''controlled-NOT'' (CNOT), whereby the logical state of the

target is flipped, $|0\rangle \leftrightarrow |1\rangle$, if the control qubit is in the logical-$|1\rangle$, and no change is made otherwise. Other examples that have no classical analog include the ''controlled-phase'' (CPHASE) and ''square-root of swap'' ($\sqrt{\text{SWAP}}$) gates [11]. In the former, the two-qubit state with both atoms in the logical-$|1\rangle$ accumulates a *phase shift* of π, $|1\rangle \otimes |1\rangle \rightarrow -|1\rangle \otimes |1\rangle$, and other local basis states remain unchanged. The $\sqrt{\text{SWAP}}$ if operated twice, exchanges the states $|1\rangle$ and $|0\rangle$; operated once we have an equally weighted superposition of no-swap and swap. These examples are entangling two-qubit gates, which together with the ability to effect arbitrary single qubit transformations, can generate an arbitrary entangled state of the many-body system through sequential pairwise application. In the language of quantum information processing, these logic gates form a universal set for quantum computation [32].

We consider the design of these logic gates for neutral atoms in tight traps (i.e., well within the Lamb-Dicke limit). We have formulated such an implementation in optical lattices [14], which offer avenues for pure quantum state preparation through resolved-sideband Raman cooling [33] and a flexible geometry for coherent control [34]. The general features apply to other traps as well, but will not be discussed explicitly here. In summary, we defined two ''species'' of atoms denoted ($\pm$), those whose light shift is dominated by the $\sigma_{\pm}$ standing wave of the lattice, respectively. Through dynamical variation of the optical lattice polarization, the two species can be brought together to interact pairwise. An auxiliary field (denoted as the ''catalysis'') excites the dipoles for the duration necessary to achieve the two-qubit logic gate. For the geometry considered in [14], we defined computational basis sets for the ($\pm$) species,

$$|1\rangle_{\pm} = |F_{\uparrow}, M_F = \pm 1\rangle \otimes |\psi_{1\pm}\rangle_{\text{ext}},$$
$$|0\rangle_{\pm} = |F_{\downarrow}, M_F = \mp 1\rangle \otimes |\psi_{0\pm}\rangle_{\text{ext}}, \tag{23}$$

where $F_{\uparrow,\downarrow} = I \pm 1/2$ are the two hyperfine levels associated with the $S_{1/2}$ ground state, M_F is the magnetic sublevel, and $|\psi\rangle_{\text{ext}}$ are the external coordinate wave functions.

For a given choice of $|\psi\rangle_{\text{ext}}$ and the catalysis field, we can define protocols for different quantum logic operations. Single bit manipulations (e.g., rotations of the qubit state on the Bloch sphere and readout of the qubit state) can be implemented through conventional spectroscopy, such as coherent Raman pulses and fluorescence spectroscopy as demonstrated in ion traps [35].

Two-qubit entanglement is achieved by inducing a conditional dipole-dipole interaction. We will consider two kinds of gates in Sec. III B. A CPHASE gate can be implemented with the following protocol. If the catalysis field is tuned near the $|S_{1/2}, F_{\uparrow}\rangle \rightarrow |P_{3/2}\rangle$ resonance with detuning small compared to the ground-state hyperfine splitting, then nonnegligible dipoles are induced *only* for atoms in the logical-$|1\rangle$ states. If there are no off-diagonal matrix elements of the dipole-dipole interaction in the chosen logical basis, and assuming the gate is performed on a time scale much faster than the photon scattering rate, this causes a nonzero *cooperative* level shift only of the logical basis state $|1\rangle_+ \otimes |1\rangle_-$, and zero cooperative level shift of all other logical basis states [see Fig. 3(a)]. Of course single atom light-shift interactions cause logical states to accumulate phase as well, but these can be removed through appropriate lights-shift pulses acting on the separated individual atoms before and after they are made to interact. If the atomic pair is allowed to evolve in the presence of the catalysis field for a time $\tau = \hbar\pi/\langle V_{dd}\rangle$ we obtain $|1\rangle_+ \otimes |1\rangle_- \rightarrow -|1\rangle_+ \otimes |1\rangle_-$ with no change to the other logical basis states, as required for a CPHASE. A similar protocol can also be constructed to implement a $\sqrt{\text{SWAP}}$ gate. Through an appropriate choice of logical basis and catalysis field, one can induce dipole-dipole couplings that are only off diagonal in the logical basis, of the type $|1\rangle_+ \otimes |0\rangle_- \leftrightarrow |0\rangle_+ \otimes |1\rangle_-$. Applying the interaction for a time such that a $\pi/2$ rotation occurs in this subspace, we obtain the desired gate [see Fig. 3(c)]. For a general initial state of the two qubits, the result of the logic gate will be an entangled state.

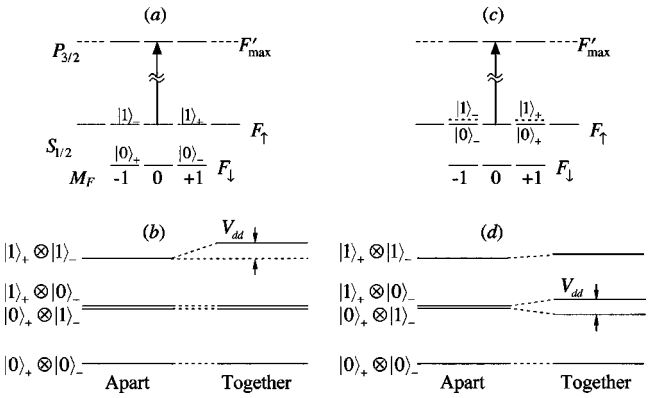

FIG. 3. Energy level structure of the logical basis associated with two-qubit logic gates. Basis states are denoted for ($\pm$) species as described in the text. (a), (b) CPHASE configuration: The ''catalysis field'' excites dipoles only in the logical-$|1\rangle$ states, chosen for both species in the upper ground hyperfine manifold $F_\uparrow$. The dipole-dipole interaction is diagonal in this basis and results solely in a level shift of the $|1\rangle_+ \otimes |1\rangle_-$ state. Operation of this gate with high fidelity requires this shift to be large compared to the cooperative linewidth. (c), (d) $\sqrt{\text{SWAP}}$ configuration. The logical basis is encoded in the vibrational degree of freedom as described in Sec. III B. For an appropriate choice of geometry and pulse timing, there is an off-diagonal coupling between the logical states $|1\rangle_+ \otimes |0\rangle_-$ and $|0\rangle_+ \otimes |1\rangle_-$, yielding a $\sqrt{\text{SWAP}}$.

The value of the figure of merit κ implies an absolute lower limit on the error probability of the quantum gate. Ignoring for the moment inelastic collisions, dissipative effects in the atomic trap, or other technical errors, imperfect fidelity is due to scattering by the catalysis field. This limit can be regarded as ''fundamental,'' in the sense that it derives from a decoherence mechanism intrinsic to our scheme. The catalysis field is present only during the entangling operation, of duration $\tau = \hbar\pi/|\langle V_{dd}\rangle|$, where the expectation value is taken in the logical $|1,1\rangle$ state. It then follows from the definition of the figure of merit, Eqs. (9) and (13), that the maximum error probability by scattering a catalysis photon is

$$P_{\text{error}} = 1 - \exp(-\Gamma_{\text{tot}}\tau) = 1 - \exp\left(-\pi \frac{\hbar\Gamma_{\text{tot}}}{|\langle V_{dd}\rangle|}\right) = 1 - \exp\left(-\frac{\pi}{|\kappa|}\right). \quad (24)$$

Assuming a large figure of merit, the error probability is approximately $P_{\text{error}} \approx \pi/|\kappa|$.

In all of the protocols, it is necessary to devise interactions that minimize loss of fidelity due to photon scattering and coherent coupling outside the logical basis (''leakage''). One leakage channel arising from the dipole-dipole potential discussed in Sec. II originates from the coherent coupling between degenerate internal states. Generally, neither M_{F1}, M_{F2} nor $M_F = M_{F1} + M_{F2}$ is conserved. From Eq. (17) we have the selection rule, $\Delta M_F = \pm|q' - q|$, where Δq is the net projection of angular momentum of the exchanged virtual photon along the atomic quantization axis. As summarized by selection rule Eq. (21), any deficit in the angular momentum of the exchanged photons must be balanced by an excitation of mechanical rotation of the two-atom molecule. If such transitions are allowed by energy conservation, they can be suppressed through judicious choice of lattice geometry. Choosing the potential to have azimuthal symmetry ensures that only the terms with $q' = q$ survive in Eq. (16), and thus $\Delta M_F = 0$. Leakage channels can also be suppressed by breaking the symmetry that leads to the degeneracy. A sufficient magnetic field can define the quantization axis, providing a linear Zeeman splitting of the ground-state magnetic atomic sublevels greater than the cooperative linewidth of these states. Processes that do not conserve the total M_F are thus detuned out of resonance [Fig. 2(b)]. Preservation of the *individual* quantum numbers M_{F1}, M_{F2} requires a nonlinear Zeeman shift of ac-Stark shift in the ground-state manifold to break the degeneracy [Fig. 2(c)].

One final leakage channel we address is coherent coupling into the excited state manifold. We must ensure that all population returns to the ground states after the logic gate is completed. One means to achieve this is to adiabatically connect the ground-manifold to the field-dressed levels. Consider the simplified basis of two two-level atoms considered in Sec. II A. Adiabatic evolution is achieved when the level splitting between the two-atom ground and first excited eigenstates, $\hbar\Delta - V_c$, is sufficiently large compared to off-diagonal coupling caused by the changing catalysis excitation. An alternative approach is to work in the opposite limit, and apply sudden pulses, fast compared to $V_{dd}/\hbar$. A real excitation is then coherently exchanged between the atoms. A similar protocol in the form of a CNOT has been proposed by Lukin and Hemmer [36] for dipole-dipole interacting dopants in a solid-state host.

B. Logic-gate protocols

In the following we describe three examples that demonstrate the flexibility available for designing quantum logic gates. We will assign a logical basis set given in Eq. (23). When the atoms are excited in phase by π-polarized catalysis light, the figure of merit is given by Eq. (13), with $q = 0$, and the atoms are super-radiant, $\Gamma_{\text{tot}} = 2\Gamma$. To complete our quantum logic protocol, we must choose the external coordinate wave function for our qubits. Considerations include maximizing the dipole-dipole figure of merit and minimizing coherent leakage due to degeneracies.

Let us first consider the case of two atoms in the vibrational ground state sharing a common well. Though spherical wells maximize the radial overlap for atoms in their ground state, the dominant term in the interaction tensor is $f_{00} = n_2(k_L r) Y_2^0(\theta) \sim Y_2^0(\theta)/(k_L r)^3$, which is orthogonal to the isotropic relative coordinate Gaussian wave function. This multipole component is nonzero, however, for nonspherical geometries and for higher motional states of the atoms in spherical wells.

One suitable design is to use ellipsoidal wells as discussed in [14]. Consider an axially symmetric harmonic potential with two atoms in the vibrational ground state, each described by a Gaussian wave packet with widths $\Delta x = \Delta y = x_0$ and $\Delta z = z_0$. The figure of merit can be calculated numerically including radiation terms, as a function of $\eta_\perp = k_L x_0$ and $\eta_\parallel = k_L z_0$ as presented in [14]. An analytic approximation follows from Eq. (13), taking into account only the near field, yields

$$\kappa \approx -\tfrac{1}{4}\langle f_{00}(r,\theta)\rangle_{\text{ext}} = -\frac{3}{4}\int d^3x |\psi_{\text{rel}}(r,\theta)|^2 \frac{P_2(\cos\theta)}{(k_L r)^3} = \frac{1}{16\sqrt{\pi}\eta_\perp^2\eta_\parallel}\left[-2 - 3\frac{\eta^2}{\eta_\perp^2} + 3\left(\frac{\eta^3}{\eta_\perp^3} + \frac{\eta}{\eta_\perp}\right)\tan^{-1}\left(\frac{\eta_\perp}{\eta}\right)\right], \quad (25)$$

where $\eta^{-2} = \eta_\parallel^{-2} - \eta_\perp^{-2}$. Keeping $\eta_\perp$ fixed while maximizing with respect to the ratio $\eta_\parallel/\eta_\perp$ gives $\kappa_{\max} \approx -8.5 \times 10^{-3}/\eta_\perp^3$. As an example, given tight localizations $z_0 = \lambda/60$, $x_0 = \lambda/130$, corresponding to Lamb-Dicke parameters $\eta_\parallel = 0.1$, $\eta_\perp = 0.05$, we have $\kappa \approx -68$.

The relatively small figure of merit for two atoms in a common prolate ellipsoidal well can be partially attributed to destructive interference between different dipole orientations. One has $V_{dd} \sim -2d^2/r^3$ when the internuclear axis is along the polarization, and $V_{dd} \sim +d^2/r^3$ for perpendicular separations. A possible solution is to use nonoverlapping spherical wells, separated along the quantization axis by Δz. We have seen that as this separation goes to zero, the dipole-dipole interaction goes to zero. We also know that $V_{dd} \sim 1/(kr)^3$ goes to zero as the separation goes to infinity. Thus at some intermediary value of atomic separation, the interaction must be maximum. Given ground-state Gaussian wave packets of width x_0 in any direction in the isotropic wells, the state is separable in center of mass and relative coordinates. Since the wave function is azimuthally symmetric, it is valid to consider only the Y_2^0 piece of the coupling tensor as discussed in Sec. III A. The figure of merit follows as in Eq. (25),

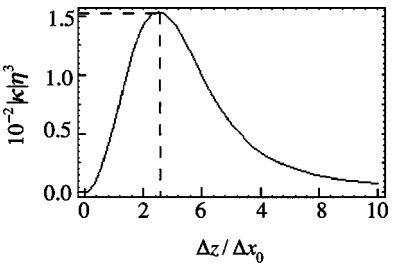

FIG. 4. Dipole-dipole figure of merit κ for spherically symmetric Gaussian wave packets with width x_0, normalized to the Lamb-Dicke parameter $\eta=kx_0$, as a function of the normalized separation $\Delta\bar{z}=\Delta z/x_0$. Maximum $|\kappa|\approx 0.015/\eta^3$ is achieved at $\Delta\bar{z}\approx 2.5$.

$$\kappa=\left[\frac{e^{-(\Delta\bar{z}/2)^2}}{\sqrt{\pi}}\left(\frac{1}{8}+\frac{3}{4\Delta\bar{z}^2}\right)-\frac{3\,\mathrm{erf}(\Delta\bar{z}/2)}{4\Delta\bar{z}^3}\right]\frac{1}{\eta^3}, \tag{26}$$

where $\Delta\bar{z}=\Delta z/x_0$, and $\eta=k_Lx_0$. The form of Eq. (26) can be verified in two limits. For $\Delta z\gg x_0, \kappa\rightarrow -0.75(k_L\Delta z)^{-3}$, the expected figure of merit for two-point dipoles separated by distance Δz, with dipole vectors aligned along the relative coordinate vector. For $\Delta z\ll x_0$, we find $\kappa\rightarrow-(\Delta\bar{z})^2/(80\sqrt{\pi}\eta^3)$, vanishing quadratically as the separation between wells goes to zero. A plot of κ is shown in Fig. 4. The figure of merit is maximized at $\Delta z_{\max}/x_0\approx 2.5$ where $\kappa_{\max}\approx -0.015/\eta^3$. For example, at $\eta=0.05, \kappa_{\max}\approx -123$. This is almost twice as good as the scheme using overlapping ellipsoidal wells with the same minimum localization.

Higher vibrational states of overlapping spherical wells can also be used to encode the qubit for controlled logic. For instance, one quanta of vibration along z in each atom could be considered to code for the logical-$|1\rangle$. This is ill suited as a logical basis, however, because of the problem of coherent leakage. The couplings given by selection rules Eqs. (20) and (21) connect the logical basis to a seven-dimensional degenerate subspace of two vibrational quanta shared between the atoms as described in Eq. (22). Many of these couplings can be avoided if instead we choose the so-called stretched states of vibration. Consider the logical basis

$$\begin{aligned}|1\rangle_\pm&=|F_\uparrow, M_F=\pm 1\rangle\otimes|n=0,l=1,m=1\rangle,\\ |0\rangle_\pm&=|F_\uparrow, M_F=\pm 1\rangle\otimes|n=0,l=0,m=0\rangle.\end{aligned} \tag{27}$$

We choose a π-polarized catalysis field applied to the transition $|S_{1/2},F_\uparrow\rangle\rightarrow|P_{3/2},F'\rangle$ with detuning *large* compared to the oscillation frequency. This induces nearly equal dipoles for atoms in logical-$|1\rangle$ and $|0\rangle$ states [see Fig. 3(b)].

Matrix elements of the dipole-dipole operator can then be calculated using Eq. (19). Unlike the previous cases discussed, the interaction operator is not diagonal in the computational basis set, $\{|0\rangle_+\otimes|0\rangle_-, |0\rangle_+\otimes|1\rangle_-, |1\rangle_+\otimes|0\rangle_-, |1\rangle_+\otimes|1\rangle_-,\}$, but instead has the form

$$V_{dd}=\frac{7}{4}\hbar\chi\begin{pmatrix}0&0&0&0\\0&1&-1&0\\0&-1&1&0\\0&0&0&\frac{4}{7}\end{pmatrix},$$

$$\chi=\frac{-(o_{F'F}c^{F_\uparrow,1,F'}_{1,0,1})^4}{70\sqrt{\pi}\eta^3}s\Gamma. \tag{28}$$

In addition, as dictated by the selection rules of Sec. II, the dipole-dipole interaction couples the logical basis states to a subspace of states with two shared quanta, $|n_1m_1l_1\rangle\otimes|n_2m_2l_2\rangle=\{|011\rangle\otimes|011\rangle, |022\rangle\otimes|000\rangle, |000\rangle\otimes|022\rangle\}$. The matrix elements are

$$\begin{aligned}&\langle 022|\otimes\langle 000|V_{dd}|011\rangle\otimes|011\rangle\\&\quad=\langle 000|\otimes\langle 022|V_{dd}|011\rangle\otimes|011\rangle\\&\quad=-\hbar\chi/\sqrt{2},\\&\langle 022|\otimes\langle 000|V_{dd}|022\rangle\otimes|000\rangle\\&\quad=\langle 000|\otimes\langle 022|V_{dd}|000\rangle\otimes|022\rangle\\&\quad=9\hbar\chi/4,\\&\langle 022|\otimes\langle 000|V_{dd}|000\rangle\otimes|022\rangle=-5\hbar\chi/4.\end{aligned} \tag{29}$$

The couplings within the degenerate vibrational subspace of Eq. (29) describe an effective two-level system with coupling between the state $|011\rangle\otimes|011\rangle$ and the symmetric state $(|022\rangle\otimes|000\rangle+|000\rangle\otimes|022\rangle)/\sqrt{2}$. The antisymmetric state is uncoupled and ''dark'' to the interaction. The effective Rabi frequency within the coupled subspace is exactly χ, thus there is a recurrence time $\tau=\pi/\chi$ for population in the vibrational state $|011\rangle\otimes|011\rangle$. For this interaction time the unitary operator in the logical basis is

$$U=\exp(-iV_{dd}\tau/\hbar)=\begin{pmatrix}1&&0&0&0\\0&\frac{e^{i\pi/4}}{\sqrt{2}}&\begin{pmatrix}1&-i\\-i&1\end{pmatrix}&0\\0&&0&0\\0&&0&1&1\end{pmatrix}. \tag{30}$$

This is the $\sqrt{\mathrm{SWAP}}$ gate universal to quantum logic [11]. The figure of merit for this gate is

$$\kappa\approx-\tfrac{1}{4}\langle 1_+1_-|f_{00}|1_+1_-\rangle=-\frac{1}{140\sqrt{\pi}\eta^3}\approx-\frac{4.02\times10^{-3}}{\eta^3}, \tag{31}$$

which for $\eta=0.05$ gives $\kappa\approx -32$.

IV. OUTLOOK

We have explored the possibility of creating multiparticle entanglement using induced dipole-dipole interactions be-

tween pairs of alkali atoms in tight traps. This system offers good prospects for quantum control of both internal and external degrees of freedom. By designing interactions that can be selectively turned on and off through an external control field, coherent interactions between atoms can be induced with high fidelity, opening possibilities for designing quantum logic gates to perform quantum information processing tasks.

The error probability of the two-qubit logic gate, finite due to spontaneous emission, is sufficient to allow us to create entangled states of multiple atoms. This holds promise for a variety of applications in precision measurement [1] and quantum simulations [3]. Such applications are possible in the short term, based on ensemble preparation and measurement on the sparse, randomly filled lattices that are available in today's laboratory experiments. In the much longer term, the promise of universal fault-tolerant quantum computing places very strong constraints on the physical system. Specifically, fault-tolerant quantum computation demands an extremely low error probability, e.g., $P_{\text{error}} < 10^{-4}$ [37] or 10^{-3} for some models [38]. Fortunately we see possibilities for substantial improvements by extending the theoretical analysis beyond the simplifying assumptions considered up to this point.

Given the scaling arguments of Sec. II, the dipole-dipole figure of merit has the form $\kappa \sim c_\kappa / \eta^3$. One may consider the ultimate limits on these parameters as determined by practical considerations. The localization η depends on the quality of the trap and possible implementations of wave packet control, such as squeezing [39]. The parameter c_κ is specific to the details of the protocol and the approximations of our analysis. Under the assumptions of our model, c_κ is determined solely by geometry and might also benefit from wave packet engineering to maximize the relevant dipole-dipole multipole component of the relative coordinate probability distribution. More importantly, we must address the limitations of our model. For atoms separated by distances on the order of an optical wavelength, it is appropriate to consider molecular rather than atomic resonances [21]. We have avoided explicit calculation of the molecular potentials by assuming a detuning that is large with respect to the splitting of these potentials. Though this assumption greatly simplifies the analysis, it is almost certainly not the optimal operating point for the system. Furthermore, at such a large detuning approaching the hyperfine splitting of the ground state, one cannot necessarily induce a dipole only for atoms in the logical-$|1\rangle$ states as we have assumed for some protocols.

Extending our model to include molecular resonance may have substantial impact on the dipole-dipole figure of merit. For example, we have argued that for atoms in the vibrational ground state of a common isotropic spherical well, the dipole-dipole coherent interaction is zero due to destructive interference when integrating over all angles of the relative coordinate vector. However, at finite detuning, e.g., red of atomic resonance, the catalysis field will preferentially excite the attractive potential, leading to finite interaction, and an increase in the parameter c_κ. Another example is the use of subradiant states. We have implicitly assumed that our dipoles are excited in phase, leading to Dicke superradiance. However, molecular resonances exist for dipoles oscillating out of phase, which might be excited with a sufficiently intense catalysis field. This too would impact the maximum possible value of c_κ in the figure of merit.

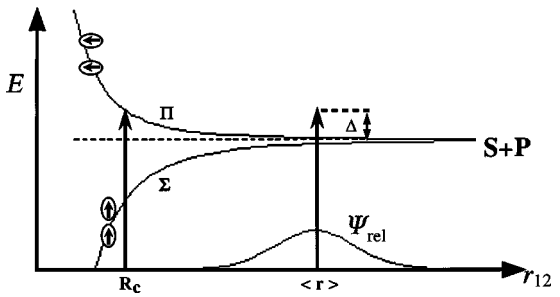

FIG. 5. Schematic of $S+P$ molecular potentials as a function of the internuclear distance r. Excitation by a far-off resonance blue detuned laser would normally be dominated by the repulsive potential at the Condon point R_C. For well localized but separated atoms (relative coordinate probability distribution sketched here) off-resonant interaction with the attractive potential dominates. The orientation of the dipoles relative to the internuclear axis is indicated for each potential.

Finally, the assumption of large detuning is brought into question when considering two atoms whose wells are closely overlapping. At some small internuclear separations, the catalysis field (as well as the trapping field, if a light trap is used) will be *resonant* with the molecular potentials—the so-called Condon point. Inelastic processes are highly probable in this case. Careful choice of the parameters may avoid these resonances over the extent of the relative coordinate probability density. In this regime off-resonant excitation dominates with an r-dependent detuning from the excited molecular eigenstates (see Fig. 5). Furthermore, the internuclear axis acquires a specific orientation with respect to the direction of the excited dipoles, and the different molecular potentials must be weighted accordingly. This is a regime not usually encountered in studies of photoassociative collisions. One future task is to include the molecular potentials in a full analysis.

Consideration of collision phenomena for atoms in tightly localized traps opens the door to a host of novel phenomena. Examples include a breakdown of the scattering length approximation for electronic ground-state s-wave scattering [40] and the production of bound molecules though photoassociation, or a transition through a Feshbach resonance [41]. Recent experiments have been performed in Bose-Einstein condensates in which colliding pairs of atoms were resonantly transferred to a bound electronic ground-state molecular resonance via Raman laser pulses [42]. This molecular bound state could act as an auxiliary level for performing a CPHASE gate by applying a 2π laser pulse between the free atom computational basis state and the molecular resonance. Whichever protocol ultimately holds the greatest promise, the rich structure of the neutral-atom/optical-lattice system provides new avenues for explorations of quantum control and information processing.

ACKNOWLEDGMENTS

We gratefully acknowledge helpful discussions with Carlton Caves, Paul Alsing, John Grondalski, and Shohini Ghose. We especially thank Gary Herling for introducing us to the Moshinski-Bracket formalism. I.H.D. and G.K.B. acknowledge support from the National Science Foundation (Grant No. PHY-9732456). P.S.I. was supported by the NSF (Grant No. PHY-9503259), by the Army Research Office (Grant No. DAAG559710165), and by the Joint Services Optics Program (Grant No. DAAG559710116).

[1] J. J. Bollinger *et al.*, Phys. Rev. A **54**, R4649 (1996). S. F. Huelga *et al.*, Phys. Rev. Lett. **79**, 3865 (1997); A. M. Childs, J. Preskill, and J. Renes, e-print quant-ph/9904021 v2.
[2] S. Lloyd, Science **273**, 1073 (1996).
[3] A. Sørensen and K. Mølmer, Phys. Rev. Lett. **83**, 2274 (1999).
[4] *Introduction to Quantum Computation and Information*, edited by H.-K. Lo, S. Popescu, and T. Spiller (World Scientific, Singapore, 1998).
[5] J. I. Cirac and P. Zoller, Phys. Rev. Lett. **74**, 4091 (1995).
[6] T. Pellizzari *et al.*, Phys. Rev. Lett. **75**, 3788 (1995). P. Domokos *et al.*, Phys. Rev. A **52**, 3554 (1995).
[7] C. Monroe *et al.*, Phys. Rev. Lett. **75**, 4714 (1995); Q. A. Turchette *et al.*, *ibid.* **81**, 3631 (1998).
[8] Q. A. Turchette *et al.*, Phys. Rev. Lett. **75**, 4710 (1995); E. Hagley *et al.*, *ibid.* **79**, 1 (1997).
[9] N. A. Gershenfeld and I. L. Chuang, Science **275**, 350 (1997). D. G. Cory *et al.*, Proc. Natl. Acad. Sci. USA **94**, 1634 (1997).
[10] S. L. Braunstein *et al.*, Phys. Rev. Lett. **83**, 1054 (1999).
[11] D. Loss and D. P. DiVincenzo, Phys. Rev. A **57**, 120 (1998).
[12] J. E. Mooij *et al.*, Science **285**, 1036 (1999).
[13] B. E. Kane, Nature (London) **393**, 133 (1998); R. Vrijen *et al.*, e-print quant-ph/9905096.
[14] G. K. Brennen *et al.*, Phys. Rev. Lett. **82**, 1060 (1999).
[15] D. Jaksch *et al.*, Phys. Rev. Lett. **82**, 1975 (1999).
[16] Q. A. Turchette *et al.*, Laser Phys. **8**, 713 (1998).
[17] A. Hemmerich, Phys. Rev. A **60**, 943 (1999).
[18] P. S. Jessen and I. H. Deutsch, Adv. At., Mol., Opt. Phys. **37**, 95 (1996).
[19] Micromagnetic traps are most promising for obtaining the tight confinement of interest here. See, for example, J. Reichel, W. Hänsel, and T. W. Hänsch, Phys. Rev. Lett. **83**, 3398 (1999), and references therein.
[20] I. H. Deutsch, G. K. Brennan, and P. S. Jessen, Fortschr. Phys., special issue on experimental proposals for quantum computation (to be published).
[21] For a review see J. Weiner *et al.*, Rev. Mod. Phys. **71**, 1 (1999), and references therein.
[22] C. J. Williams and P. S. Julienne, J. Chem. Phys. **101**, 2634 (1994); P. D. Lett, P. S. Julienne, and W. D. Phillips, Annu. Rev. Phys. Chem. **46**, 423 (1996).
[23] See, for example, C. Cohen Tannoudji, J. Dupont-Roc, and G. Grynberg, *Atom-Photon Interactions* (Wiley-Interscience, New York, 1992), pp. 585–589.
[24] J. Guo and J. Cooper, Phys. Rev. A **51**, 3128 (1995); E. V. Goldstein, P. Pax, and P. Meystre, *ibid.* **53**, 2604 (1996).
[25] P. S. Julienne, Phys. Rev. Lett. **61**, 698 (1988).
[26] R. H. Lemberg, Phys. Rev. A **2**, 883 (1970); M. Trippenbach, B. Gao, J. Cooper, and K. Burnett, *ibid.* **45**, 6555 (1992).
[27] E. U. Condon and G. H. Shortley, *The Theory of Atomic Spectra* (Cambridge University Press, Cambridge, 1935).
[28] C. Cohen-Tannoudji, B. Diu, and F. Laloe, *Quantum Mechanics* (Hermann, Paris, France, 1977), Vol. 1.
[29] M. Moshinsky, Nucl. Phys. **13**, 104 (1959).
[30] See EPAPS Document No. E-PLRAAN-61-077006 for the calculation of the tensor coupling between two particles occupying a common spherical well. Dipole-dipole interaction matrix elements for up to two quanta shared between two atoms are tabulated therein. This document may be retrieved via the EPAPS homepage (http://www.aip.org/pubservs/epaps.html) or from ftp.aip.org in the directory /epaps/. See the EPAPS homepage for more information.
[31] T. A. Brody, G. Jacob, and M. Moshinsky, Nucl. Phys. **17**, 16 (1960).
[32] A. Barenko *et al.*, Phys. Rev. A **52**, 3457 (1995).
[33] S. E. Hamann *et al.*, Phys. Rev. Lett. **80**, 4149 (1998); H. Perrin *et al.*, Europhys. Lett. **42**, 395 (1998); A. J. Kerman *et al.*, Phys. Rev. Lett. **84**, 438 (2000).
[34] I. H. Deutsch and P. S. Jessen, Phys. Rev. A **57**, 1972 (1998); M. Morinaga *et al.*, Phys. Rev. Lett. **83**, 4037 (1999).
[35] For a review of experiments that perform quantum coherent manipulations of trapped ions, see D. J. Wineland *et al.*, J. Res. Natl. Inst. Stand. Technol. **103**, 259 (1998).
[36] M. D. Lukin and P. R. Hemmer, Phys. Rev. Lett. **84**, 2818 (2000).
[37] J. Preskill, Proc. R. Soc. London, Ser. A **454**, 385 (1998).
[38] C. Zalka, e-print quant-ph/9612028.
[39] S. Marksteiner *et al.*, Appl. Phys. B: Lasers Opt. **B60**, 145 (1995).
[40] M. Olshanii, Phys. Rev. Lett. **81**, 938 (1998); E. Tiesinga, C. J. Williams, F. H. Mies, and P. S. Julienne (unpublished).
[41] F. Mies, E. Tiesinga, and P. S. Julienne, Phys. Rev. A **61**, 022721 (2000).
[42] R. Wynar *et al.*, Science **287**, 1016 (2000).